Naval Research Laboratory
Washington, DC 20375-5320

NRL/FR/7140--97-9842

Bottom Scattering Strengths Measured in Deep and Shallow Water Using the Deep Towed Acoustics/Geophysics System

JOSEPH JEFFERY
PETER M. OGDEN

Acoustic Systems Branch
Acoustics Division

April 30, 1997

REPORT DOCUMENTATION PAGE

Form Approved
OMB No. 0704-0188

1. AGENCY USE ONLY (*Leave Blank*)	2. REPORT DATE	3. REPORT TYPE AND DATES COVERED
	April 30, 1997	Final Report, 1994-1996

4. TITLE AND SUBTITLE

Bottom Scattering Strengths Measured in Deep and Shallow Water Using the Deep Towed Acoustics/Geophysics System

5. FUNDING NUMBERS

PE - 62435N
DN-16-3740

6. AUTHOR(S)

Joseph Jeffery and Peter M. Ogden

7. PERFORMING ORGANIZATION NAME(S) AND ADDRESS(ES)

Naval Research Laboratory
Washington, DC 20375-5320

8. PERFORMING ORGANIZATION REPORT NUMBER

NRL/FR/7140--97-9842

9. SPONSORING/MONITORING AGENCY NAME(S) AND ADDRESS(ES)

Office of Naval Research (Code 32)
Arlington, VA 22217

10. SPONSORING/MONITORING AGENCY REPORT NUMBER

11. SUPPLEMENTARY NOTES

12a. DISTRIBUTION/AVAILABILITY STATEMENT

Approved for public release; distribution unlimited.

12b. DISTRIBUTION CODE

13. ABSTRACT (*Maximum 200 words*)

The Deep Towed Acoustics/Geophysics System (DTAGS) has been used for some years by Naval Research Laboratory investigators to examine the structure of ocean-bottom sediments. With the replacement of the DTAGS horizontal array by a vertical array, it became possible to use the system to measure bottom scattering strengths in both deep and shallow water. The first DTAGS scattering measurements with the vertical array were taken in two general locations: in deep water near the Mid-Atlantic Ridge, and in shallow water near the Hudson Canyon. Analysis of the deep-water results shows scattering strengths from a thickly sedimented area to be somewhat lower than Mackenzie scattering levels, with a relatively flat dependence on grazing angle. The scattering strengths decrease slightly as frequency increases from 300 to 540 Hz, consistent with other measurements of this type. Scattering strength measurements were successfully carried out in shallow water as well. Although aspects of the data collection led to low confidence in the absolute levels, the feasibility of the low-frequency measurement approach was demonstrated.

14. SUBJECT TERMS

Low-frequency acoustics
Shallow water
Scattering strengths
Bottom scattering

15. NUMBER OF PAGES

25

16. PRICE CODE

17. SECURITY CLASSIFICATION OF REPORT	18. SECURITY CLASSIFICATION OF THIS PAGE	19. SECURITY CLASSIFICATION OF ABSTRACT	20. LIMITATION OF ABSTRACT
UNCLASSIFIED	UNCLASSIFIED	UNCLASSIFIED	UL

NSN 7540-01-280-550

Standard Form 298 (Rev. 2-89)
Prescribed by ANSI Std 239-18
298-102

CONTENTS

BOTTOM SCATTERING STRENGTHS MEASURED IN DEEP AND SHALLOW WATER USING THE DEEP TOWED ACOUSTICS/GEOPHYSICS SYSTEM

INTRODUCTION

The accurate prediction of reverberation levels in littoral waters for active acoustic systems requires substantial information about the nature and acoustic properties of the ocean bottom. In deep water, the overall reverberation background from an active system will only occasionally be dominated by bottom reverberation; in slope and shallow water environments, bottom reverberation is expected to be the most important contributor to the noise background.

The state of understanding of acoustic bottom reverberation is significantly behind that of surface and volume reverberation. Part of the reason for this is the difficulty of making measurements of both low-frequency bottom backscattering strengths and supporting geophysical properties at the same site, particularly in shallow water. Unfortunately, many geophysical measurements get easier as water depth decreases, while bottom backscatter (and forward scatter) measurements become more difficult. This difficulty is due to the number of parasitic ray paths that interfere with the ability to obtain a "clean" measurement of backscatter. For this reason, at present there are very few measurements of low-frequency bottom scattering strengths in shallow water, and even fewer that are accompanied by much geophysical information.

The difficulty of measuring bottom backscattering strengths means that new ways of making these measurements are of considerable interest. This paper is concerned with examining one such new method, the use of the Deep Towed Acoustics/Geophysics System (DTAGS). This system, a ship-towed multichannel seismic system developed by Gettrust and co-workers at the Naval Research Laboratory-Stennis Space Center, Mississippi, has been used and continues to be used as a means of probing the structure of ocean bottom sediments (see for example, Gettrust and Ross 1990). The addition of a vertical line array (VLA) to the existing DTAGS horizontal array and omnidirectional source has improved the capabilities of the system for measuring bottom backscattering. The use of a VLA results in a nearly monostatic measurement and gives a more straightforward geometry compared to a horizontal array. This combination of arrays offers the potential advantage of being able to obtain backscattering strengths and geophysical data at nearly the same time and same place. The DTAGS VLA was first used to collect acoustic data during the Acoustic Reverberation Special Research Program (ARSRP) experiment over the Mid-Atlantic Ridge in July 1993. Following the ARSRP test but on the same cruise, DTAGS was deployed in shallow water near Hudson Canyon off New Jersey. At both sites, the deployment of DTAGS was made from the R/V *Knorr*.

The acoustic data collected from these two deployments have been examined to verify the viability of DTAGS for measuring bottom backscattering strengths in both shallow and deep water. This report has two goals:

- to document the analysis methods used with these data sets to obtain scattering strengths,
- to present backscattering strengths measured with the DTAGS vertical array.

Manuscript approved February 27, 1997

This is the first time this system has been used to obtain such measurements. Therefore we have concentrated our analysis efforts primarily on the deep-water data set because it provides fewer potential complications than the shallow-water data set. In addition, some of the same VLA data we analyzed from the Mid-Atlantic Ridge has also been examined by Tang et al. (1995) for similar purposes; this provides a means of comparing the results of two different analysis methods.

SYSTEM DESCRIPTION AND EXPERIMENT GEOMETRY

In its original configuration, DTAGS consists of a single omnidirectional Helmholtz transducer at the head of a horizontal towed array. For a typical measurement, the source and receiver are deployed to within a few hundred meters of the water-sediment interface and are towed slowly over the bottom. The source sends out frequent linear frequency-modulated signals (LFMs) that penetrate into the sediment to depths of several hundred meters, with the reflected returns received on the towed array. These returns are then analyzed to give the density and sound-speed structure of the subbottom at a spatial resolution up to about 5 m.

In the new configuration used for the measurements analyzed in this paper, the horizontal towed array was replaced by a vertical array deployed below the omnidirectional source. Figure 1 is a schematic of the geometry. The vertical array had 24 elements spaced at 2-m intervals, which meant that the array was cut for 375 Hz. The top element of the array was located 56 m below the Helmholtz transducer. During the experiments, the transducer sent out 0.125-s LFM up-chirps over a frequency range of 250 to 650 Hz, with a 30-s interval between chirps. The approximate source level of the transducer was 185 to 190 dB re 1 μPa @ 1 m

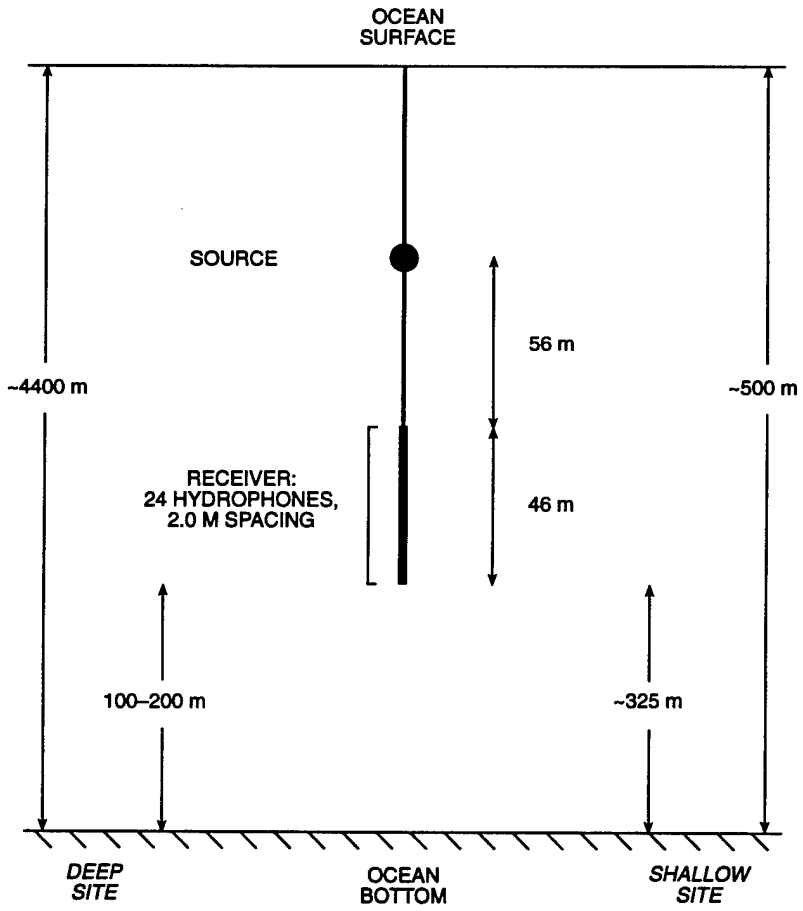

Fig. 1 — DTAGS measurement geometry

(Rowe 1995). The data were recorded on the *Knorr* at a sampling rate of 2314.8 samples/s, well above the Nyquist rate for all frequencies analyzed. A highpass filter at 50 Hz eliminated low-frequency interference. DTAGS was used in a "sprint and drift" mode during the tests, with the ship drifting at 0.25 m/s or less while acquiring data.

As noted previously, bottom scattering data were obtained at two sites during and after the ARSRP test. The first set of measurements was carried out in July 1993 over the Mid-Atlantic Ridge, near 26°10′N, 46°8′W (hereafter referred to as the deep site). Figure 2 is a DBDB5 bathymetry map of the area. The water depth in this location is approximately 4400 m. (Note that the DBDB5 database plotted in Fig. 2 has the depth incorrect near the experiment site. DBDB5 should be used only for the most schematic representations of bathymetry, such as showing the relative positions of test sites.) The measurements were made over a "sediment pond," a flat-bottomed region that Tang et al. characterize as having a top layer of calcareous mud, with sediment thicknesses ranging from near zero at the edges of the pond to about 430 m at the center. During these measurements, DTAGS was positioned between 100 and 200 m (measured from the bottom hydrophone) above the sea floor. This meant that returns from the sea surface were not important for the analysis, as they came in too late to be of consequence. The actual distance of the array above the bottom was determined for each data set by the timing of the pulse after reflection off the bottom.

The second set of measurements was taken near Hudson Canyon, in the general vicinity of 39°17′N, 72°22′W (hereafter referred to as the shallow site). Figure 3 is a DBDB5 bathymetry map of the area. These measurements were carried out over the Continental Slope, so that the water depth varied from roughly 270 to 850 m for the positions at which we analyzed data. According to an examination by Fulford (1997) of sediment data from two Amcor drill holes (612 and 621) in the vicinity of the canyon, the sediment at the shallow site appears to consist of a thin layer (of order 15 m) of calcareous silt overlying at least 300 m of predominantly clay intermixed with some sand.

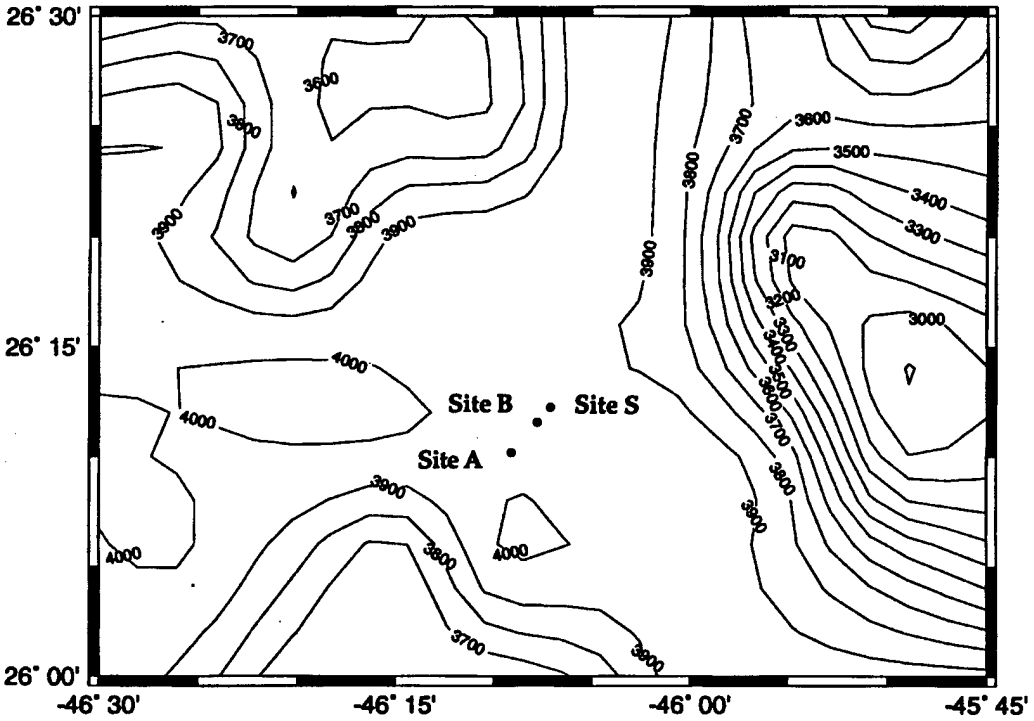

Fig. 2 — DBDB5 bathymetry map of the Mid-Atlantic Ridge ("deep site") showing the locations of the measurements. Bathymetry contour are in meters.

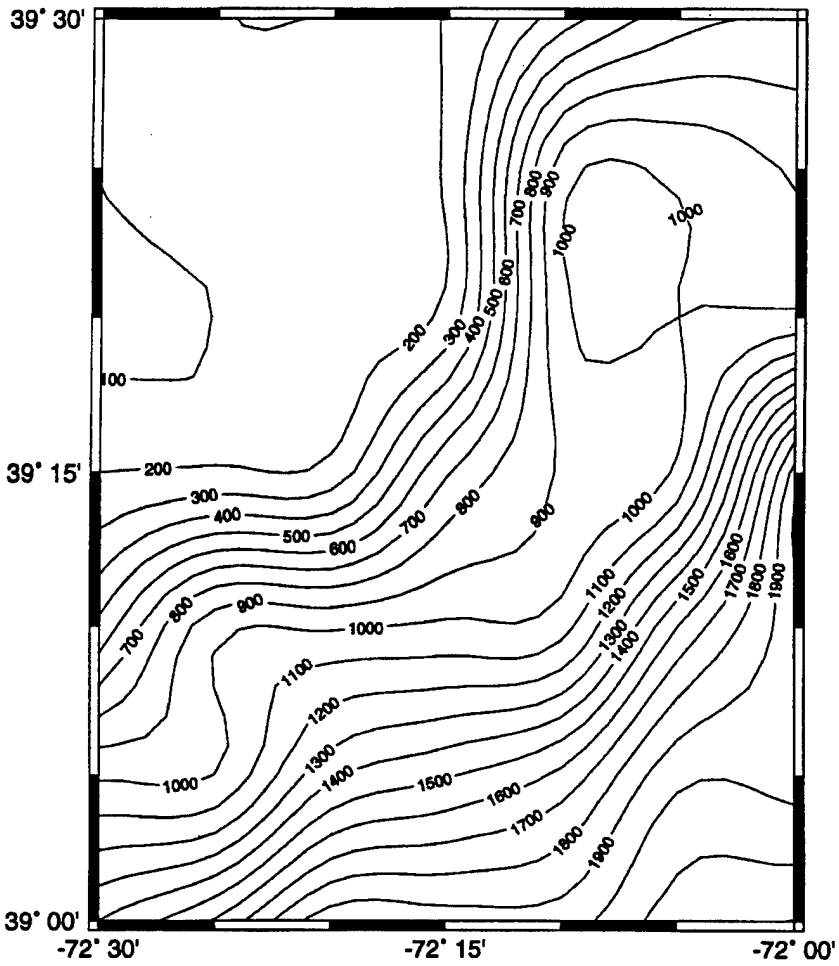

Fig. 3 — DBDB5 bathymetry map of the Hudson Canyon ("shallow site"). Bathymetry contours are in meters.

The array was kept at a constant depth of 75 m (measured from the source) during the shallow-site measurements because of concerns about array safety. Although the distance of the array from the surface could be determined unambiguously from the timing of the reflected pulse, the identification of the bottom-reflected pulse proved somewhat problematic. Particularly at the shallowest depths examined, the upward-moving pulse was occasionally difficult to identify clearly, probably because of the distance of the array from the bottom (and the consequent low signal power) and the confusion of interfering returns. Figure 4 shows an example of shallow-water returns from the top and bottom hydrophones. Examining consecutive chirps and waterfall plots of all the hydrophones was sometimes helpful in identifying the fathometer returns. Overall, however, the determination of exact bottom depths at the shallow site was not very precise.

One additional factor that had to be considered at both sites was the tilt of the vertical array. The tilt could be estimated by timing the transmitted and bottom-reflected pulses at the top and bottom hydrophones. It was found that the differences in timing were smaller than our measurement accuracy, which implied that the tilt was smaller than about 5 deg. We therefore assumed that the tilt was zero for all measurements.

DATA ANALYSIS

Because of the wide bandwidth and short duration of the transmitted signal, we decided to use two different methods to process the data: matched-filter processing and spectral processing. For the matched-

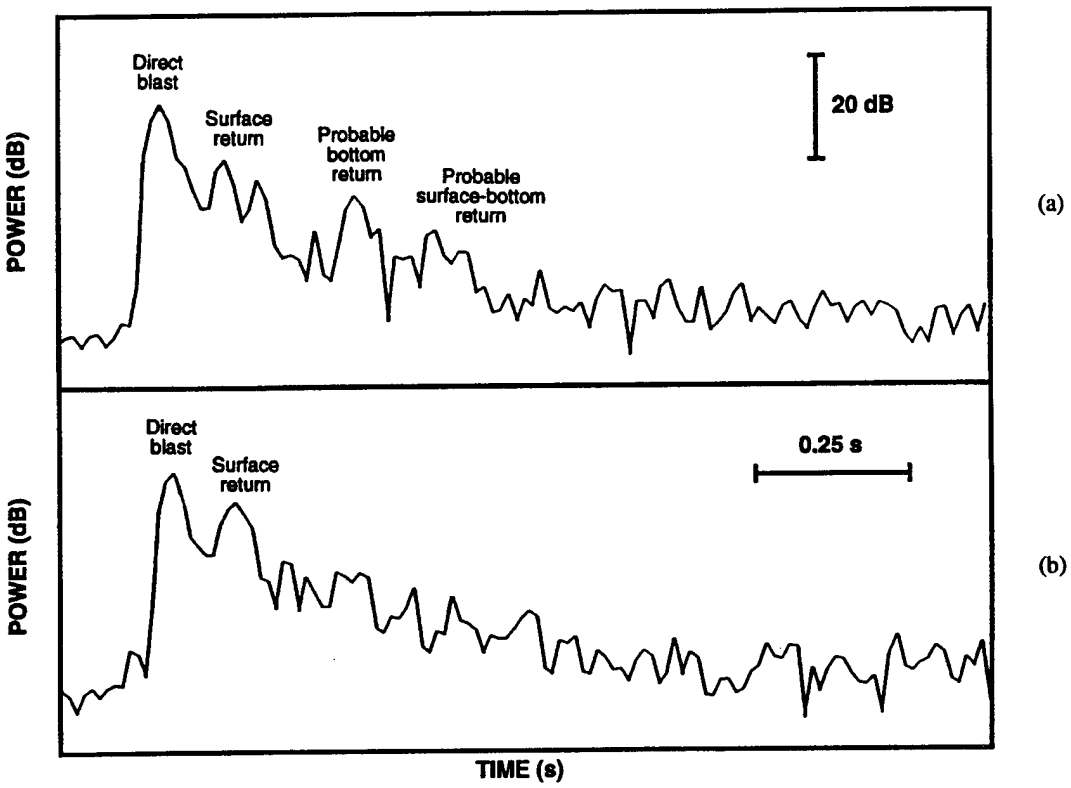

Fig. 4 — Examples of shallow-water returns: (a) Top hydrophones (b) Bottom hydrophones

filter approach, we analyzed the LFM as four separate, 80 Hz waveforms (with algebraic centers at 300, 380, 460, and 540 Hz) by using four different matched filters with different transmission times. For the spectral processing, we treated the broadband signal as a series of impulses that were translated into the frequency regime by a fast Fourier transform (FFT) and then analyzed as if they were short continuous-wave signals.

The Appendix provides details of the data analysis, so only a brief overview of the process is given here. After a set of about eight good pings had been selected at each site, beamforming was done on each ping using a Hamming-weighted, 18-hydrophone subaperture of the VLA. Nineteen cosine-spaced beams were formed, running from upward endfire (beam 0) to downward endfire (beam 18). The pings were then averaged together to produce a single reverberation curve for each beam and frequency. A raytrace program was used to calculate the geometrical parameters of the scattering process, such as grazing angles, insonified areas, and transmission losses. Finally, the reverberation curves were combined with the source level and the geometrical factors to solve the sonar equation for scattering strength as a function of frequency, grazing angle, and site.

RESULTS

Deep Site Results

We have calculated scattering strength results for three deep positions over the ARSRP sediment pond. The positions (and their arbitrarily assigned names) are

- site A: 26°10.0′N, 46°8.6′W;
- site B: 26°12.0′N, 46°7.5′W; and
- site S: 26°12.2′N, 46°7.3′W.

Site A is near the center of the sediment pond; sites B and S are closer to the northeast edge of the pond. All are in water depths of about 4400 m. In each case, about eight pings were combined into one average reverberation curve that was used to calculate scattering strengths. The uncertainty in the results due to ping-to-ping variability is ±2.5 to 3 dB. Overall uncertainty in the deep-site results caused by this variability and other factors (such as source level determination) is of order ±4 dB.

The matched-filter results for site A are shown in Figs. 5 to 8. Each of these figures presents results for one of the four analysis bands, and each contains the results for four different beams. In addition, each of these plots (and all other scattering strength plots in this paper) has the Mackenzie scattering curve (Lambert's law with a frequency-independent coefficient of –27 dB) plotted as a reference. The main response axes for the beams (beam 0 is the upward endfire beam, beam 9 is broadside) are beam 10: 96 deg, beam 11: 103 deg, beam 12: 110 deg, and beam 13: 116 deg.

The scattering strengths measured at site A are generally below the Mackenzie scattering levels, but with a different grazing-angle dependence. In all four frequency bands, the scattering strengths show a flatter dependence on grazing angle than the $\sin^2\theta$ dependence of Mackenzie-Lambert scattering. This type of behavior has been observed from other low grazing-angle observations in this type of sediment (Holland et al. 1996). Furthermore, comparison of Figs. 5 through 8 shows a frequency dependence in the scattering strengths such that scattering levels decrease as frequency increases. This also is consistent with other observations of scattering from thickly sedimented areas.

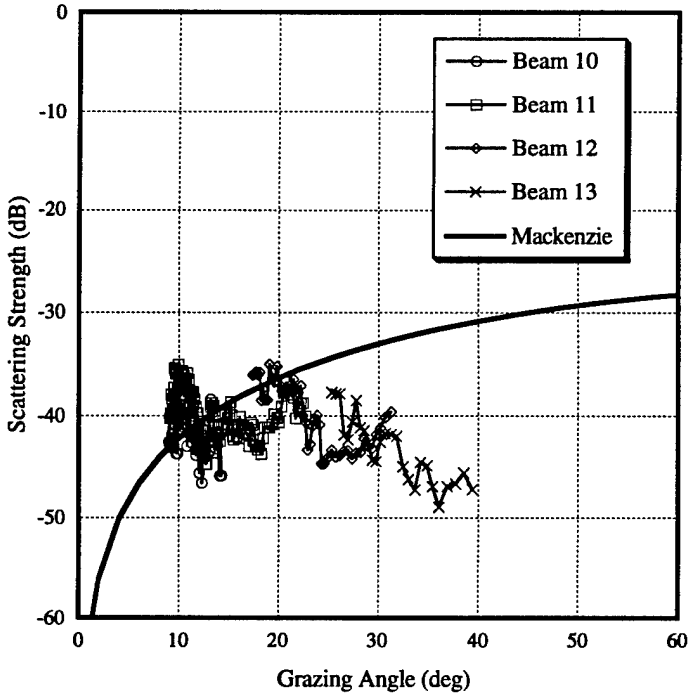

Fig. 5 — Matched-filter scattering strength results at 300 Hz for site A

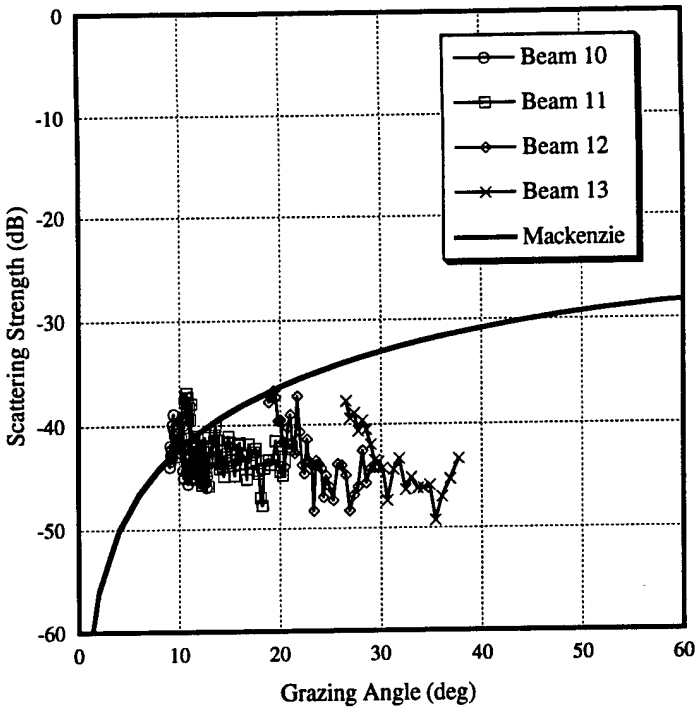

Fig. 6 — Matched-filter scattering strength results at 380 Hz for site A

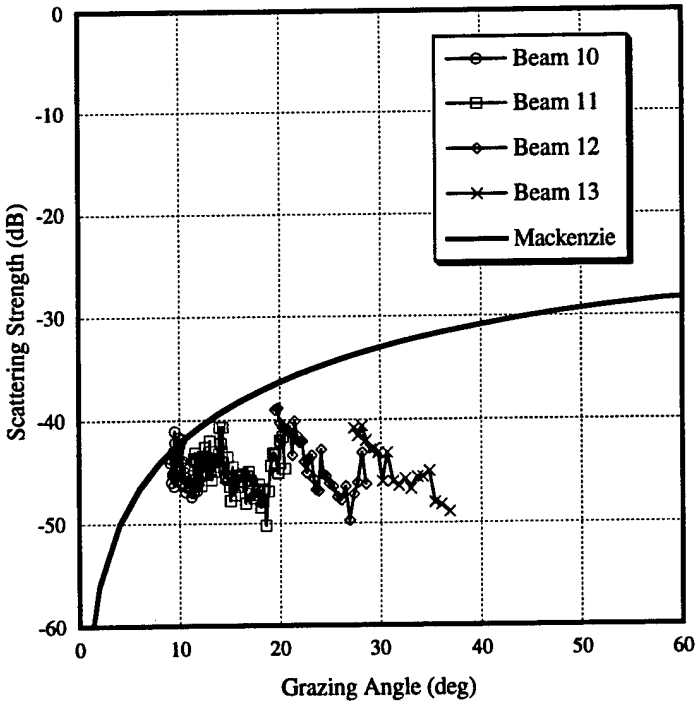

Fig. 7 — Matched-filter scattering strength results at 460 Hz for site A

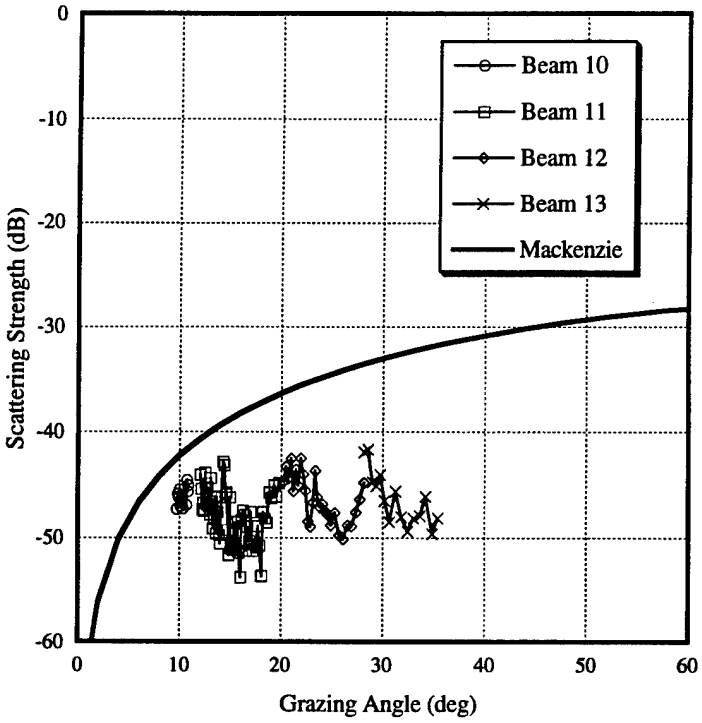

Fig. 8 — Matched-filter scattering strength results at 540 Hz for site A

Based on the type of past experience discussed by Holland et al., the most reasonable interpretation of this result is that the scattering is coming from either inhomogeneities deep within the sediment or from the basement. The frequency dependence is then due to attenuation within the sediment rather than any inherent frequency dependence of the scattering mechanism. The scattering levels appear to be too high to be reasonably interpreted as coming from sediment/interface scattering (Mourad and Jackson 1993). Tang et al. also interpret the scattering from this area as being caused by volume inhomogeneities within the sediment rather by than sediment/interface scattering. The levels measured by Tang et al. are somewhat higher than are shown in Figs. 5 through 8, and have a grazing-angle dependence much closer to Lambert's law than our results. However, they are examining scattering from specific layers within the sediment over the full bandwidth of the signal and are also looking mostly at higher grazing angles than we are. Holland et al. have discussed the idea that scattering strengths measured at different grazing angles using different methods should not be routinely extrapolated. Without a more detailed geoacoustic model, it is not possible to say for certain whether our results and those of Tang et al. should be in agreement. Certainly they are not inconsistent with each other, and both sets of results lead to the conclusion that interface scattering is not important for these conditions.

Comparison of the site A matched-filter results with those computed using spectral processing shows very good agreement, reinforcing confidence in the matched-filter processing technique. Figure 9 shows a sample of the spectral-processing results, which gives site A scattering strengths at 388 Hz. In general, the spectral-processing results are generally somewhat noisier than the matched-filter results, probably due to the smaller bandwidth and energy being processed.

Site B was closer to the edge of the sediment pond than to the center, and according to Tang et al. the thickness of the sediment was substantially less. The scattering strength results for site B, presented in Figs. 10 through 13, show evidence of this thinner sediment layer. At 300 Hz, the curves in Fig. 10 not only are substantially higher overall than the corresponding 300 Hz results at site A, but they show more evidence of

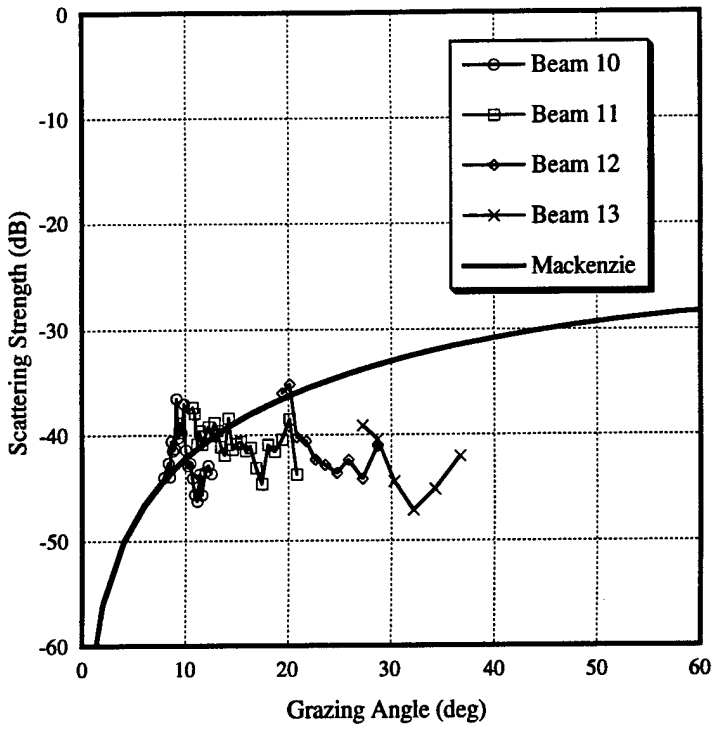

Fig. 9 — Spectral-processing scattering strength results at 388 Hz for site A

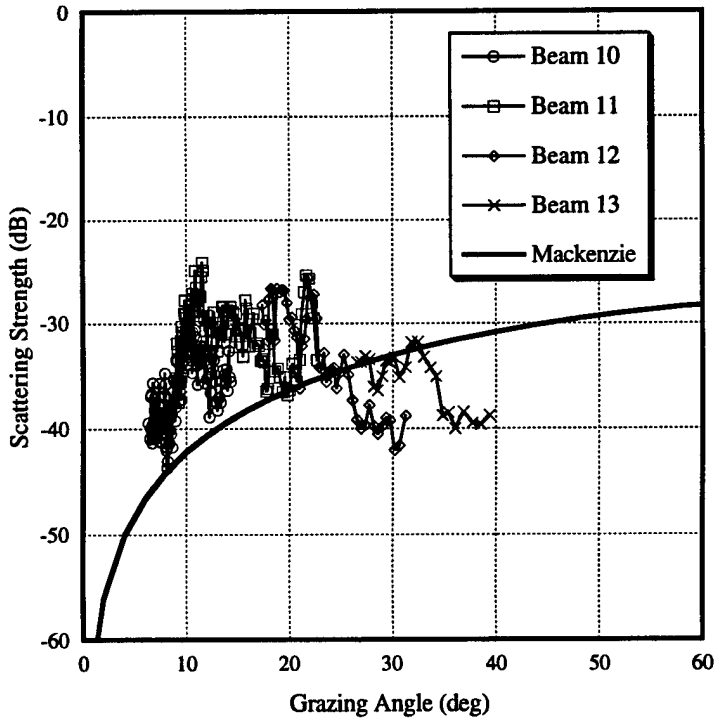

Fig. 10 — Matched-filter scattering strength results at 300 Hz for site B

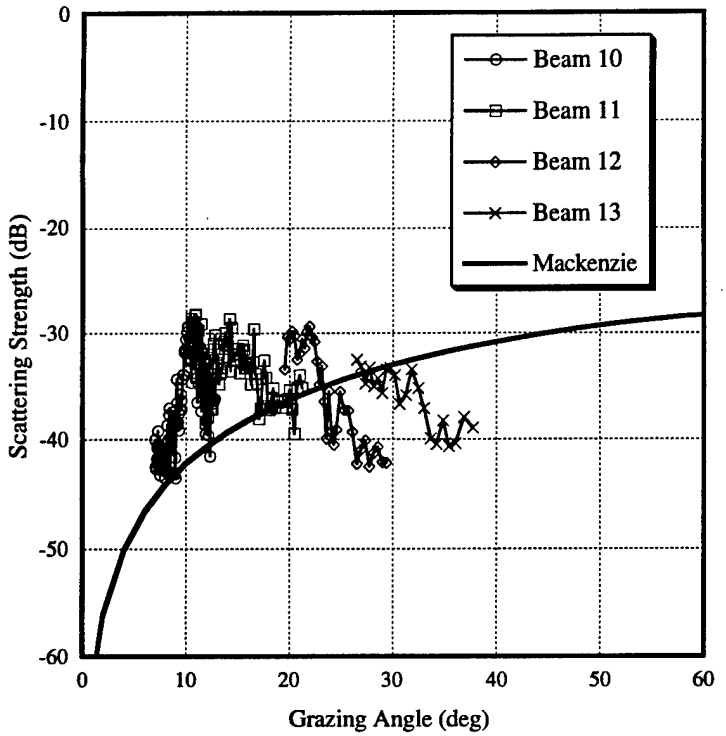

Fig. 11 — Matched-filter scattering strength results at 380 Hz for site B

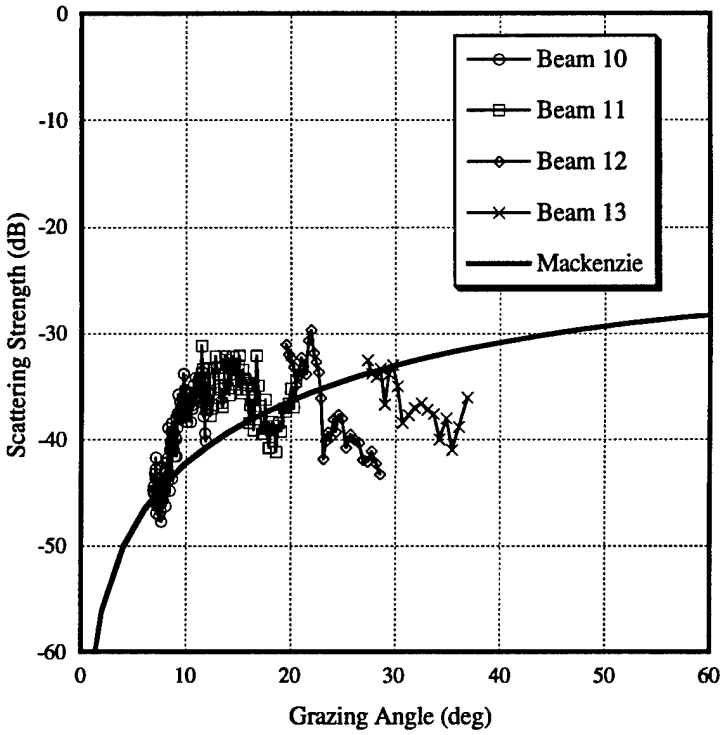

Fig. 12 — Matched-filter scattering strength results at 460 Hz for site B

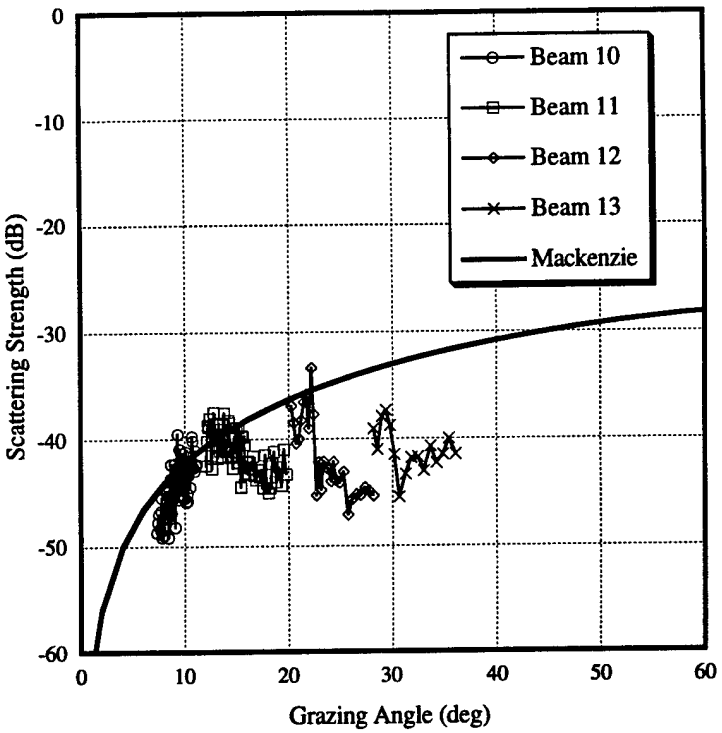

Fig. 13 — Matched-filter scattering strength results at 540 Hz for site B

scattering from discrete layers, such as the features around 22 and 12 deg. As the frequency increases, these features decrease in strength, as do the overall scattering levels. This is consistent with the idea that the scattering is dominated by interaction with strong acoustic horizons (perhaps the basement) embedded in the sediment, with attenuation responsible for the observed frequency dependence. At the very lowest grazing angles measured, the scattering strengths show a pronounced decline at all frequencies, beginning around 10 deg. This may be the result of the energy no longer interacting with the strong scattering layer due to the sediment sound speed structure, leaving the (much lower) scattering that comes from within the volume of the sediment (see Holland et al. for a discussion of this effect). As at site A, the spectral-processing results are similar to the matched-field results, so no examples are presented.

The results for site S are given in Figs. 14 through 17. Site S is relatively close to site B, and the results show the same basic characteristics as those from site B: enhanced scattering levels, the presence of individual features, and a decrease in scattering strengths as frequency increases. It should be noted that, due to the details of the geometry at this site, beam 10 does not contribute many points, so the low grazing angles are not present. Again, the spectral-processing results are similar.

Shallow Site Results

We have also examined data from the vicinity of the Hudson Canyon, in relatively shallow water. As discussed in both the body of this report and in the Appendix, the results obtained from this area are subject to substantial uncertainties because of the difficulty in specifying the exact geometry and the lack of in situ sound speed profiles. In addition, the greater distance of the source and receiver from the bottom caused the shallow-water data to have a significantly lower signal-to-noise ratio; enough lower, in fact, that at a site with a water depth of 500 m, there effectively were no scattering results at the higher DTAGS frequencies.

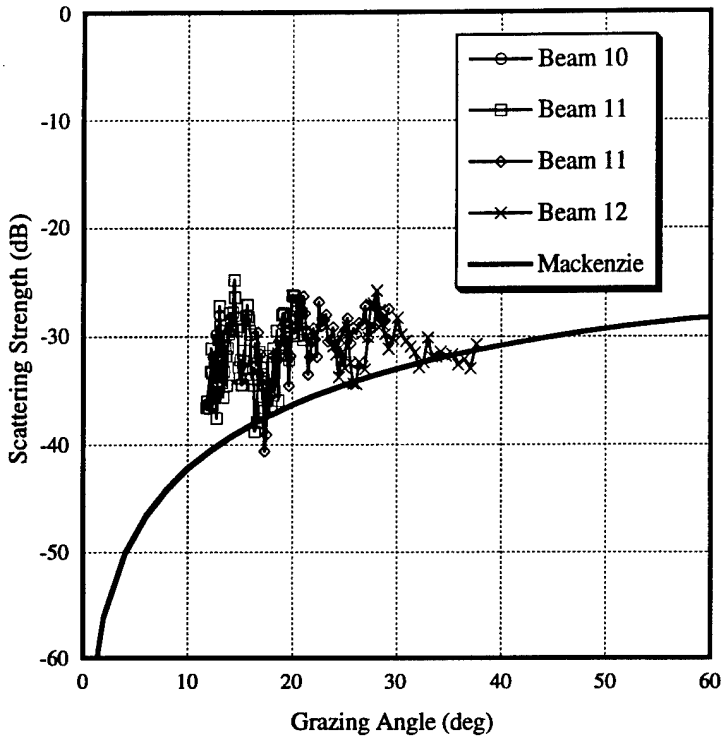

Fig. 14 — Matched-filter scattering strength results at 300 Hz for site S

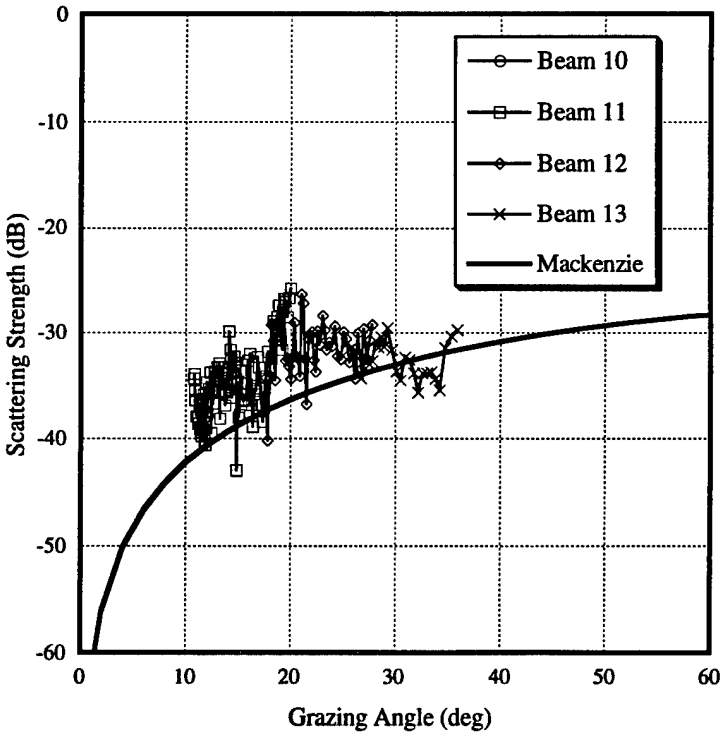

Fig. 15 — Matched-filter scattering strength results at 380 Hz for site S

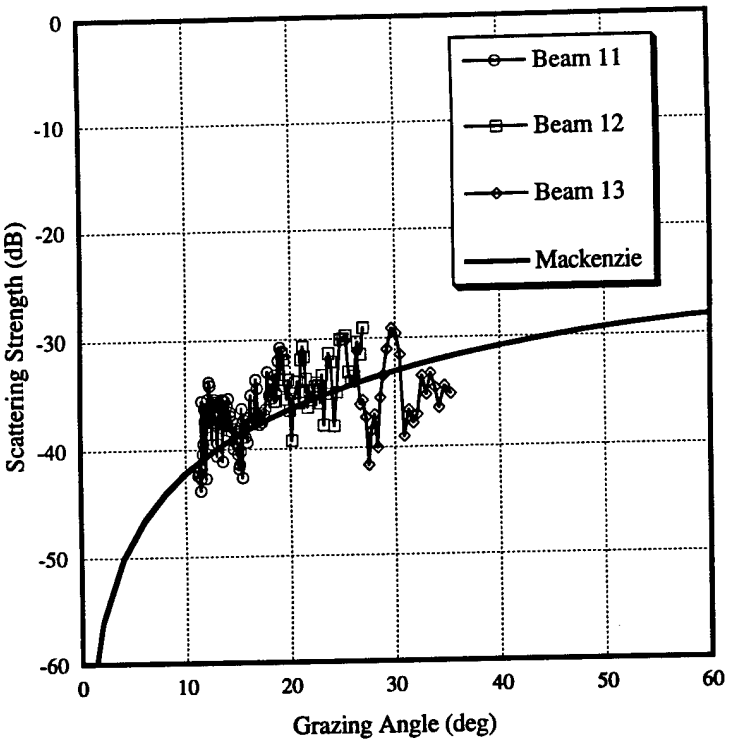

Fig. 16 — Matched-filter scattering strength results at 460 Hz for site S

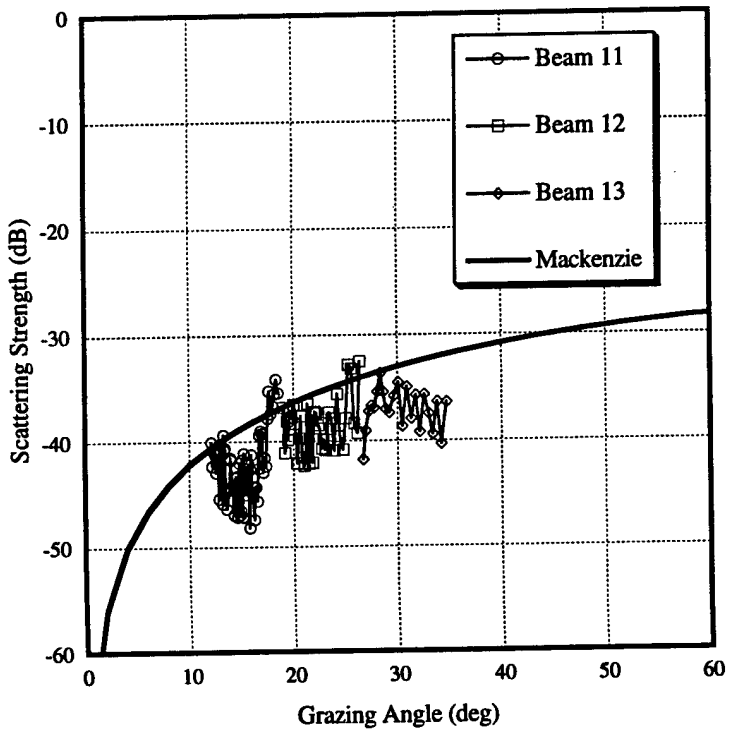

Fig. 17 — Matched-filter scattering strength results at 540 Hz for site S

In spite of these factors, however, measurements of this type appear to be feasible in littoral waters. Examples of the results from the 500-m site are shown in Figs. 18 through 20. These figures show scattering strengths for the lower three matched-filter analysis bands. In addition to the beams used in deep water, these figures include results from beams 14 (124 deg) and 15 (132 deg), as near-field considerations do not come into play for the geometry used. As may be expected, the higher grazing-angle results appear to be dominated by residual fathometer returns, which cause the scattering strengths above about 40 deg to increase rapidly with increasing grazing angle. There is a curious feature at about 30-32 deg that either represents a "notch" of some kind or, more likely, indicates that the scattering below 30 deg is being dominated by some other effect than that causing the scattering above 30 deg. (This notch was present in other data sets from nearby regions that were examined.)

Two additional points should be made: first, the results show no significant frequency dependence at this site, in contrast to the deep-water data. The lack of frequency dependence may mean that scattering is coming from fairly high in the sediment column, which is consistent with the relatively high scattering levels. However, the range of frequencies measured is not very large, so it could be that there is a weak frequency dependence that we are not seeing in these data. In general, frequency dependence at DTAGS frequencies is thought to come from attenuation in the sediment. Its absence suggests either very low attenuation in the Hudson Canyon sediments or a primary scattering center that is not deeply imbedded. Additional geophysical information would be very useful for resolving this issue. Second, there does not appear to be a problem with interference from fathometer returns at the lower grazing angles. This is encouraging from the point of view of being able to carry out other shallow-water measurements using similar systems.

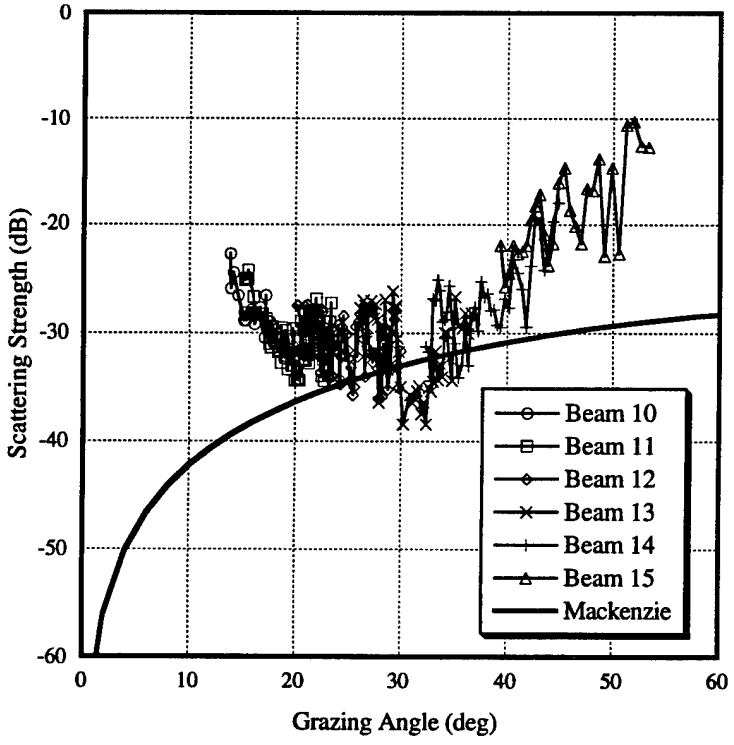

Fig. 18 — Matched-filter scattering strength results at 300 Hz for the shallow site

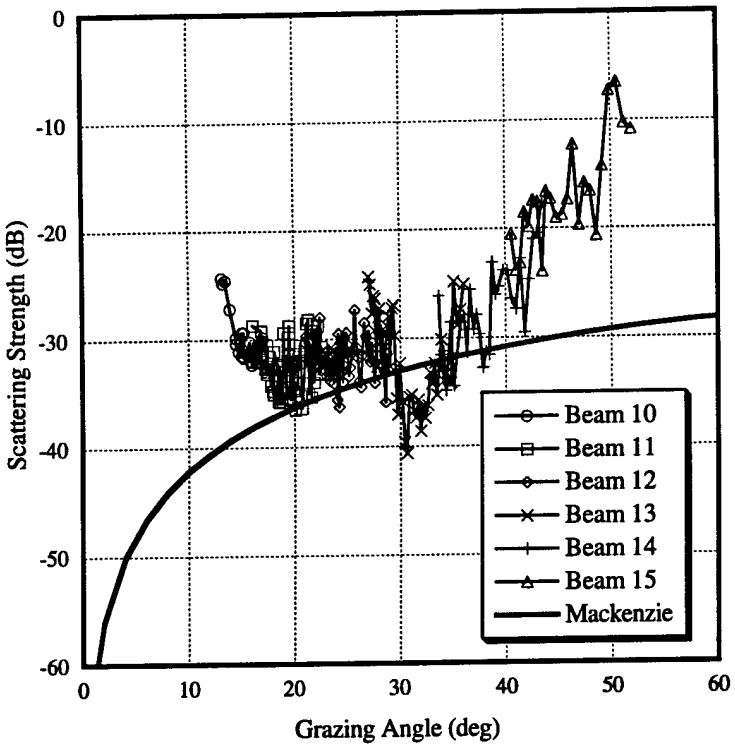

Fig. 19 — Matched-filter scattering strength results at 380 Hz for the shallow site

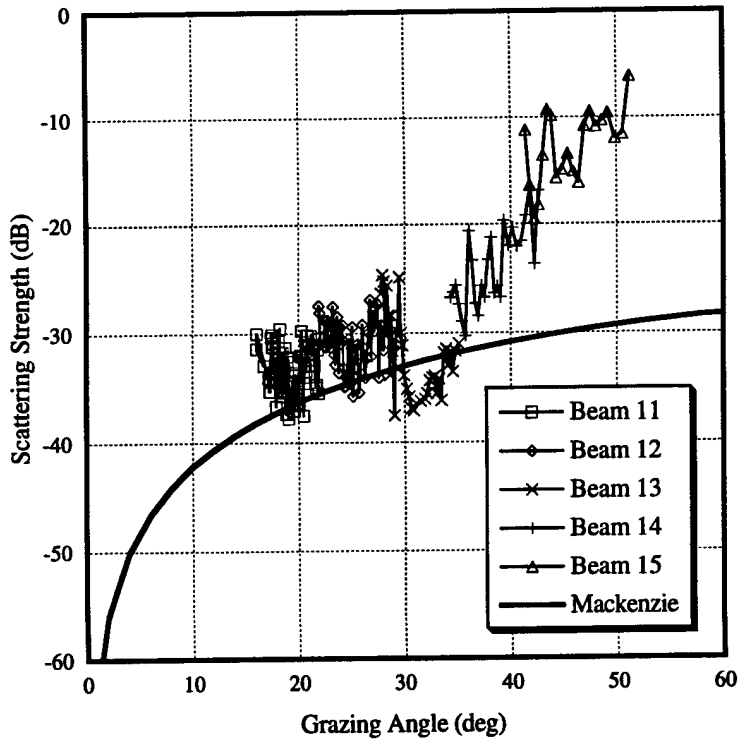

Fig. 20 — Matched-filter scattering strength results at 460 Hz for the shallow site

SUMMARY AND RECOMMENDATIONS

The vertical array configuration of DTAGS was used for the first time during the ARSRP experiment to collect data from which bottom scattering strengths could be derived. We have analyzed these data from several deep- and shallow-water sites and have obtained scattering strengths over a frequency range from 300 to 540 Hz and at grazing angles from as low as 7 deg up to about 40 deg.

For the sites at the Mid-Atlantic Ridge sediment pond, the results were typical of those found in other areas with similar sediment composition. The overall scattering levels were below the Mackenzie scattering levels, with scattering strengths decreasing as frequency increased. The grazing angle dependence was somewhat flatter than that of Lambert's law, again similar to measurements made at other sites. The results are consistent with scattering dominated by subbottom effects rather than the water/sediment interface, particularly in areas where the sediment was not very thick. Strong evidence of basement scattering was seen in the thinner-sediment cases. The observed frequency dependence was probably controlled by absorption within the sediment.

At the shallow-water sites near the Hudson Canyon, we successfully extracted scattering strengths from the data for several different water depths. However, measurement uncertainties and experiment design features led to the shallow-water results having substantially lower confidence levels than the deep-water results. It was possible to draw some conclusions about the scattering, however, most notably that there seemed to be little frequency dependence and that fathometer returns did not appear to be a strong source of interference at these sites. The principal conclusion from the shallow-water analyses is simply that such measurements are feasible using as system such as the vertical-array DTAGS.

Finally, it is clear that the interpretation of bottom backscattering strengths requires a good geophysical model, primarily for two reasons. First, geophysical data can establish where the scatterers are likely to be. This can be combined with the measured scattering strengths to form a self-consistent picture of the scattering environment. Second, the measurement process is inextricably tied up with the measurement results, so that almost any measurement is likely to have some system-dependent effects. The only way to remove these effects is to have a good acoustic model that takes into account not only the geophysical structure of the scattering area, but also the specific geometry of the experiment. This is especially true when the source is omnidirectional, which results in many paths in the sediment that could contribute to the scattering.

Based on our experience with this analysis effort, we make the following recommendations and observations for future measurements:

- Given the substantial variability of conditions in littoral waters, it is extremely important to obtain in situ measurements of the supporting environmental data, most crucially sound speed in the water.

- Large-bandwidth FM signals are usable for measuring scattering strengths, but a series of short CWs covering the same frequency range would probably be better for making measurements. For the short time scales involved in measurements taken near the bottom or in shallow water, waveforms that allow pulse compression do not have any particular advantages that outweigh the long pulse lengths.

- Time needs to be built into the recording scheme for the noise background to be measured prior to each ping.

- Signal-to-noise considerations require that the system be placed nearer to the bottom than occurred during the series of measurements described here. In order to do this in littoral waters and still ensure array safety, the deploying platform will need to have a depth-measurement capability, presumably a fathometer.

- Using signals at a frequency higher than that for which the receiving array was cut was not a problem for this set of measurements as the beams being analyzed were close to broadside, and the results were confined to low grazing angles. If higher grazing angles were desired, spatial aliasing on the array could become an issue.

ACKNOWLEDGMENTS

This work was funded by the Office of Naval Research, Code 32. We thank Joseph Gettrust and Mary Rowe (NRL-Stennis Space Center) for supplying us with the data and supporting information, as well as for useful insights made during the analysis process. We also thank Joseph M. Fialkowski and Jerome C. Richardson (Planning Systems, Incorporated) for assistance with the analysis and for many helpful discussions about signal processing, and Roger Gauss and David Fromm (NRL-DC) for assistance with the paper.

REFERENCES

J.K. Fulford, NRL-SSC, private communication (1997).

J.F. Gettrust and J.H. Ross, "Development of a Low-Frequency, Deep-Towed Geoacoustics System," Proceedings of Ocean '90: IEEE, 38-40 (1990).

C.W. Holland, P.M. Ogden, M.T. Sundvik, and R. Dicus, "Critical Sea Test Bottom Interaction Overview," CST White Paper, Space and Naval Warfare Systems Command (PMW-182), SPAWAR CST/LLFA-WP-EVA-46, September (1996).

P.D. Mourad and D.R. Jackson, "A Model/Data Comparison for Low-Frequency Bottom Backscatter," *J. Acoust. Soc. Am.* **94**, 344–358 (1993).

M. Rowe, "Calibration of the DTAGS Source and Estimation of Deep-Ocean Ambient Noise," NRL-SSC draft memorandum (1995).

D. Tang, G.V. Frisk, C.J. Sellers, and D. Li, "Low-frequency Acoustic Backscattering by Volumetric Inhomogeneities in Deep-Ocean Sediments," *J. Acoust. Soc. Am.* **98**, 508–516 (1995).

Appendix

DATA ANALYSIS METHODS

Figure A1 shows the overall data processing path used to analyze the DTAGS data. The processing steps are summarized as follows: (1) converting data from UNIX-recorded units to VAX integers; (2) basebanding and filtering data; (3) assessing data quality; (4) beamforming a subaperture of the vertical array; (5) either matched-filtering or FFTing the data; and (6) combining the measured reverberation curve with the calculated geometric parameters of the experiment to solve the sonar equation for scattering strengths as a function of grazing angle and beam. The remainder of this section gives details on each of these steps.

The first task in the analysis was to convert the recorded data from a UNIX storage format to a VAX format. This involved using a byte-swapping algorithm followed by conversion to files with restructured headers. After the data were in suitable format, the individual phone time series were put through what is called first-pass processing in the NRL processing suite. In first-pass, 256 data samples were put through a 512-element FFT to get into the frequency domain. The outputs of the FFT were then multiplied by a finite impulse-response (FIR) bandpass filter to isolate the bandpass of interest and allow for a smooth inverse FFT later on in the processing. The FIR filter used for the DTAGS processing had 130 coefficients and rolloff points of 198.9 and 650.9 Hz (for a 452 Hz effective processing bandwidth). By keeping only the data in the frequency bins from 135.6 to 714.2 Hz, the data were basebanded with a new sampling rate of 578.6 samples/s. This reduced the size of the files used in the processing without any loss of information.

After transforming the data into the frequency domain and filtering, the next processing step was to assess the quality of the data. Examination of the deep-site data showed that as many as half the pings were corrupted by an interfering signal of unknown origin. Examples of both good and bad pings are shown in Fig. A2. During the corrupted pings, a "hump" showed up at random times that often was as strong as the fathometer returns. Figure A3 shows examples of FFT spectra from the direct blast and the interfering hump. The two are clearly distinct in their frequency character. It is possible that the hump came from cable strum. More likely, however, it originated from another test or experiment being carried out at the same time as the DTAGS test. In any case, any pings that contained this particular contaminating feature were rejected from the ensemble.

For shallow-site data, other interference problems limited the useful data set. The lower hydrophones were found to have random spikes in their signals. (As is discussed later, because the analysis was done on a subaperture of the VLA, this problem was dealt with by using only the upper hydrophones.) A number of the ping recordings terminated early, probably because of some bit errors. When insufficient time after a transmission was available, the ping was rejected for use in the analysis. Examination of the data showed that there were occasional substantial increases (as much as 15 to 20 dB) in the level of ambient noise, which were most likely caused by ship thrusters used to correct for ship's drift. Finally, the tow ship was found to have a strong harmonic in the vicinity of 360 Hz, which made analysis near that frequency impossible.

In spite of these interference problems, it was straightforward to assemble a good-quality data set at each of the sites. The good pings were very reproducible. We generally used about eight pings in each data set to produce the final results.

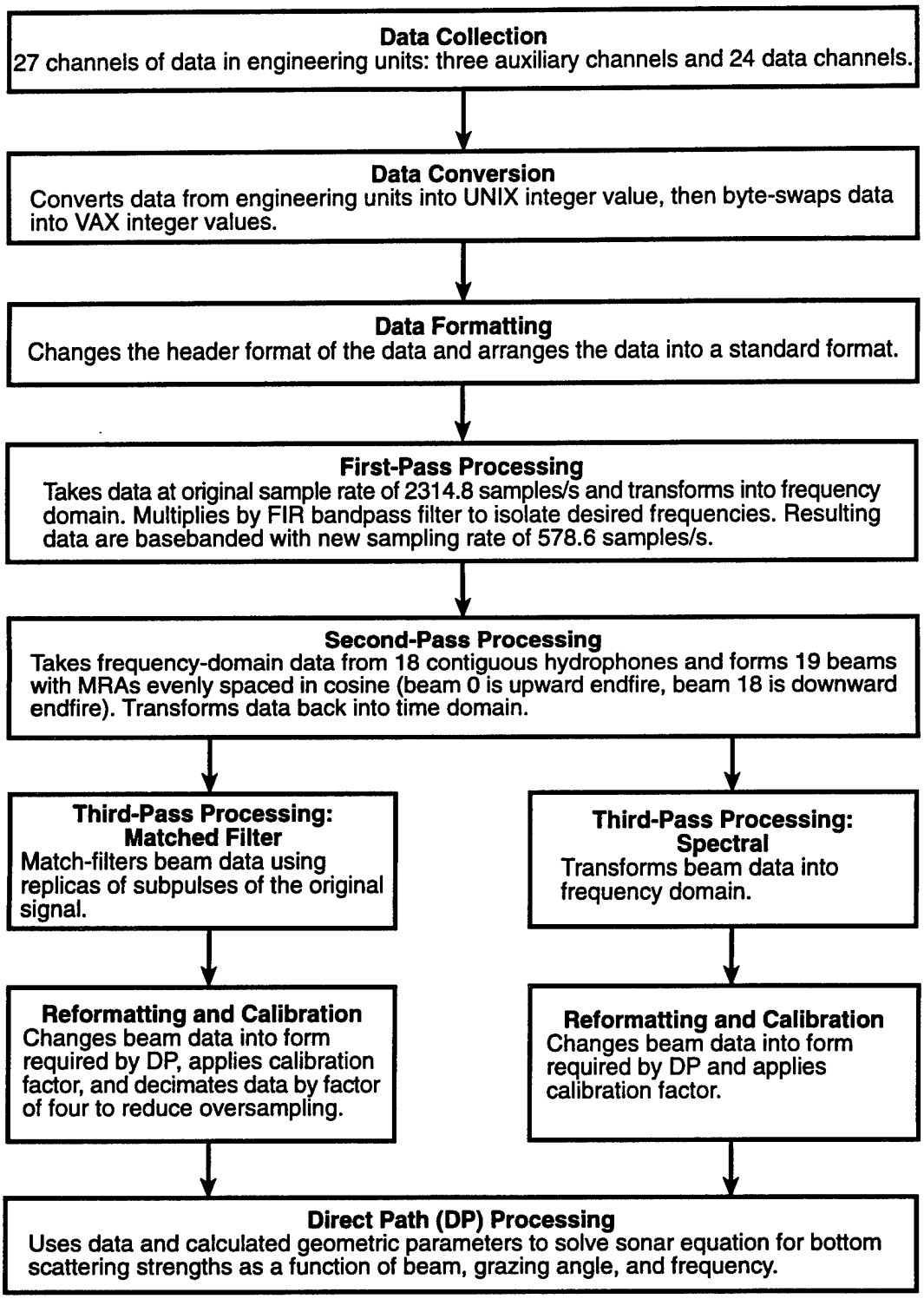

Fig. A1 — Processing path followed for DTAGS analysis

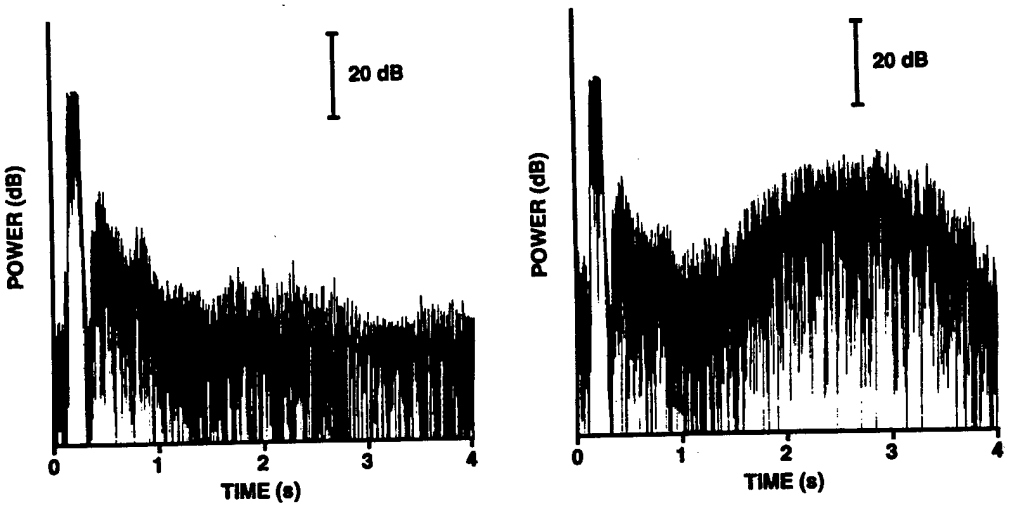

Fig. A2 — Examples of deep-water time series showing a) uncorrupted and b) corrupted ping

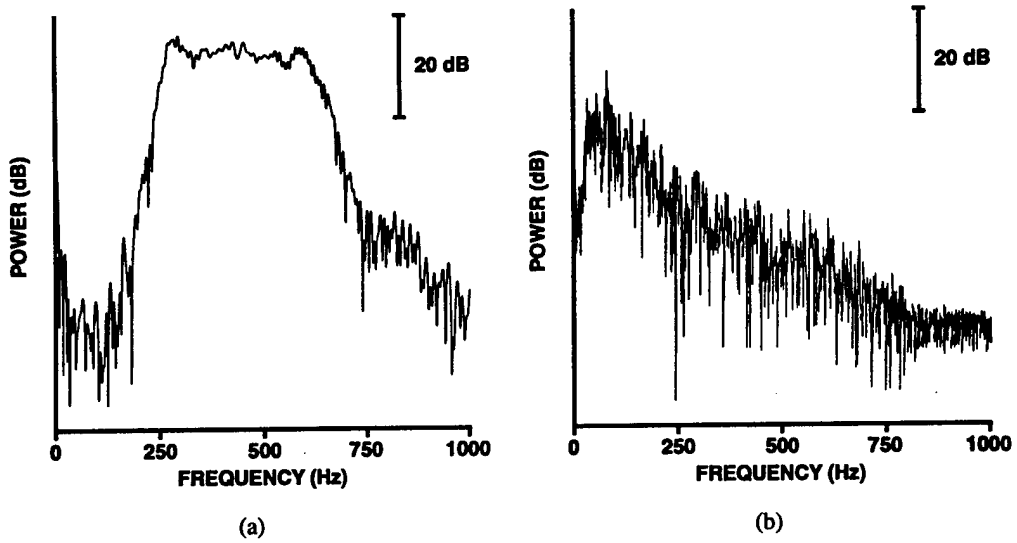

Fig. A3 — Frequency characteristics of a) direct blast and b) "hump"

Once a reasonable set of pings had been selected, the hydrophone data were beamformed in the frequency domain (referred to as second-pass processing). Although data were recorded on 24 hydrophones, near-field considerations and the interference problems referred to previously led us to use an 18-phone subaperture for the beamforming. (At the deep site, the center 18 were used; at the shallow site, the top 18 were used.) Nineteen beams were formed for each data set, running from top endfire (beam 0) to bottom endfire (beam 18). The beam pointing directions were evenly spaced in cosine and were formed using Hamming shading. Because the array had a design frequency of 375 Hz, some of the beams formed from the subaperture were subject to spatial aliasing at the higher analysis frequencies. However, the beams on which the analysis was conducted were near broadside. For these beams, theoretical beam pattern plots suggested that there were no aliased sidelobes of any consequence.

The next stage of the normal NRL processing operation is converting the beam frequency data into beam time series data. This is done by calculating an inverse FFT using the same number of points (512) as the direct FFT. One reason for doing this is that the basebanded, filtered time series files are significantly smaller than the original time series data files, although for the DTAGS data the reduction in file size was not of major importance. Another, more relevant reason for converting back into the time domain is to produce a single set of files that can be used as inputs for both matched-filter processing and spectral processing without having to do first- and second-pass processing for the matched-filtered and spectral-processing files individually. Because of the conversion back into time series data, the original, arbitrary choice of FFT length does not affect any subsequent processing.

When the inverse FFTs had been calculated, the processing of the DTAGS data divided into two tracks: matched-filter processing and spectral processing. The motivation for using two different processing schemes was that the DTAGS source signal was designed for geophysical processing and was not optimal for acoustic scattering measurements. If the entire 400 Hz bandwidth (BW) LFM were to be match filtered, the resulting effective footprint of the waveform on the bottom (1/400 s, or a linear distance of about 2 m) is less than a wavelength in size. Because scattering strength is normally thought of as an averaged quantity, this seemed to be an unreasonably small bottom sample, even taking into account the averaging around an annulus. The best solution was to break the LFM into subpulses, which would also have the advantage of allowing the frequency dependence of the bottom scattering to be examined over the bandwidth of the signal. However, careful choices of subpulse bandwidths had to be made. Poor choices could result in effective ping lengths that were so short that some of the assumptions that cause matched-filter processing pulse compression to be valid would be violated. The compromise values that we adopted for bandwidth and subpulse duration appeared to satisfy these concerns.

Because of the considerations outlined above, we decided to analyze the 400 Hz LFM as four subpulses, each with an 80 Hz bandwidth: 260-340 Hz, 340-420 Hz, 420-500 Hz, and 500-580 Hz. Note that for an 80 Hz pulse, the length of the pulse-compressed resolution element (1/BW) is 0.0125 s, while the length of the 80 Hz subpulses is 0.025 s, thereby satisfying (barely) the conditions for the validity of pulse compression. (The crossover point for the DTAGS signal is a bandwidth of 56 Hz, at which the two lengths are equal.) After the data were match filtered, the levels were corrected by a factor of 10 log(BW) to take into account the pulse compression.

As a check on the matched-filter processing, we also processed the data using spectral processing techniques. This involved selecting small bandwidths of the signal and treating them as if they were impulses at a constant frequency. For this approach, we used 128 samples of data in the FFTs (i.e., 0.22 s of data), which gave frequency resolution bins of 4.5 Hz. We then averaged four bins together to get reverberation levels averaged over 18 Hz.

Because of some issues in the interpretation of the source level, we calculated the scattering results through the use of a self-calibration technique. Self-calibration can be used when the source and receiver are in a known geometry so that the transmission loss from source to receiver can be calculated with confidence. It also depends on the direct blast not being clipped at the hydrophone. Both these conditions were satisfied for the DTAGS geometry. To calibrate the data at a particular frequency, an arbitrary calibration constant is assumed and applied to the data. The reverberation data are then examined to determine the level of the direct blast at the hydrophone. The (known) transmission loss is then added to the direct-blast level to get the source level. Whatever assumptions were made in the choice of the calibration constant were also made in the source level, and since the source level is subtracted from the reverberation level in the sonar equation,

the assumptions cancel. We used this method to determine the source level for each of the matched-filter bands as well as each of the spectral-processing bands. We also examined multiple hydrophones to verify the assumptions regarding hydrophone clipping and the predictability of the transmission loss. We found that the source level was relatively flat as a function of frequency, as Gettrust (1995) had found during his source characterizations.

The remainder of the processing was done by the Direct Path (DP) software analysis package. DP has been described in detail elsewhere (Ogden and Erskine 1994), so only a brief description of it is given here. The functions of DP are: to allow the selection of a consistent data set; to calculate all the geometrical parameters involved in the scattering process; and to solve the sonar equation for scattering strength using the measured beam reverberation curves, the source level, and calculated geometric parameters. The output of DP is scattering strength as a function of frequency, beam, and time. The time dependence is converted into grazing angle dependence by assuming that the scattering comes from the water-sediment interface and identifying the grazing angle for a given time since the beginning of the ping. (It has become increasingly clear [see, for example, Holland et al. 1996] that scattering at DTAGS frequencies does not, in fact, originate at the water-sediment interface, but rather from within the sediment volume. The assignment of grazing angle using this assumption is a method used by most investigators, however.)

For the DTAGS data, DP modeled the receiver geometry as a cylindrically symmetric (i.e., zero-tilt) vertical array with Hamming-shaded beams originating from the center of the subaperture. At the deep site, measured sound speed profiles were available for use in calculating the geometric parameters like transmission loss, incident and scattered grazing angles (nearly identical for this geometry), and insonified area. At the shallow site, however, the only measured profiles were from a site many miles away from the measurement location. They were judged to be inadequate, so we had to use archival profiles from the GDEM (Generalized Digital Environmental Model) sound speed database in the analysis. This is potentially a substantial source of error. For this reason and others already discussed, the shallow-site results should be treated primarily as a demonstration of the effectiveness of the technique rather than as reliable measurements of bottom backscattering.

A final analysis issue is the estimate of the noise level as a function of frequency and beam. DP usually uses a period of time prior to the ping as a source of the noise level, which is then subtracted from the total reverberation to get the net reverberation. (The cutoff for the scattering strength calculations is when the total reverberation is 3 dB above the noise background.) Because the DTAGS system only records 4 s of data beginning shortly before the ping time, there was generally insufficient time before the ping to get a good noise estimate. We therefore took the noise from the last half-second of the data series. This may still have had some residual reverberation in it, but in general this time appeared to be adequate for estimating a true noise level.

REFERENCES

J.F. Gettrust, NRL-SSC, private communication (1995).

C.W. Holland, P.M. Ogden, M.T. Sundvik, and R. Dicus, "Critical Sea Test Bottom Interaction Overview," CST White Paper, Space and Naval Warfare Systems Command (PMW-182), SPAWAR CST/LLFA-WP-EVA-46, September (1996).

P.M. Ogden and F.T. Erskine, "Surface Scattering Measurements Using Broadband Explosive Charges in the Critical Sea Test Experiments," *J. Acoust. Soc. Am.* **95,** 746–761 (1994).

M. Rowe, "Calibration of the DTAGS Source and Estimation of Deep-Ocean Ambient Noise," NRL-SSC draft memorandum (1995).